

# Molecule-Frame Photoelectron Angular Distributions from Oriented CF<sub>3</sub>I Molecules

Peter Downie and Ivan Powis\*

*School of Chemistry, University of Nottingham, Nottingham NG7 2RD, United Kingdom*

(Received 21 September 1998)

Electron-ion recoil vector correlations in dissociative  $5a_1^{-1}$  photoionization of CF<sub>3</sub>I are examined with a photoelectron-photoion coincidence imaging technique and fixed-molecule photoionization calculations. The CF<sub>3</sub><sup>+</sup> dissociation channel results are readily interpreted as molecule-frame photoelectron angular distributions from, effectively, oriented parent molecules. The competing I<sup>+</sup> fragmentation channel distributions, while similar at higher ionization energies, deviate nearer to the I<sup>+</sup> dissociation threshold, revealing nontrivial (non-axial-recoil) ion fragmentation dynamics in this region. [S0031-9007(99)08870-5]

PACS numbers: 33.80.Eh, 33.60.Cv, 34.80.Kw

Measurements of molecule-frame photoelectron angular distributions (PADs) have the potential to provide a very powerful probe of the photoionization dynamics [1]. In marked contrast to established lab-frame PAD measurements (where averaging over random initial molecular orientation reduces the information content to just a single anisotropy parameter,  $\beta$ ), molecule-frame PADs may be richly structured and afford access to the  $l$ -resolved amplitudes and phases of the scattered photoelectron. While this approach therefore offers a route towards a dynamically “complete” molecular photoionization experiment, progress in pursuit of this desirable goal has been somewhat limited due to the difficulty of obtaining an oriented, gas-phase molecular sample.

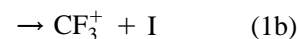
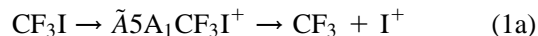
One promising approach is *via* the determination of electron-fragment ion recoil vector correlations observed in dissociative photoionization. Such correlations were first remarked upon in photoelectron-photoion coincidence experiments as unexpected fragment ion time-of-flight distributions [2] which, it was argued, could reveal information on the fixed-molecule PAD [3,4]. It was subsequently possible to confirm by experiment predictions of a reversal in the direction of the molecule-frame PAD caused by shape-resonance induced  $l$ -dependent phase shifts in PF<sub>3</sub> [5,6]. An adapted coincidence technique, employing a rotatable detector to examine directly the angular distribution, was demonstrated by Golovin [7] and has been further applied by Shigemasa *et al.* to study core level ionization in small molecules [8,9].

The principle behind these experiments is as follows: both the photoelectron ejection and subsequent dissociation of the residual parent molecular ion core are dynamical fragmentation processes which are expected to have characteristic angular distributions in the molecular coordinate frame. Hence some mutual correlation of the recoil vectors may be anticipated. However, while the electron distribution is expected to demonstrate quantum interferences, the heavier molecular fragments may well behave more classically. In particular, in the axial-recoil limit the ion fragment is assumed to recoil along a single well-

defined direction, corresponding to the instantaneous direction of the fragmenting bond [10]. Assuming the two fragmentation processes to be effectively sequential steps, and both to be more rapid than the characteristic molecular rotational period, a simple interpretation of the angular correlation results; namely, that the distribution of  $\chi$ , the angle between electron and ion recoil vectors in the center-of-mass frame, is just the photoelectron angular distribution referred to the molecular axis. A fixed-molecule PAD is thus obtained not by imposing an initial preferred orientation on the randomly oriented gas phase sample, but rather by inferring the orientation of individual molecules from their subsequent ion fragment recoil direction.

In this Letter, we present the first quantitative fixed-molecule PADs obtained for the valence shell ionization of a polyatomic molecule. Such valence results may ultimately be more sensitive to the *molecular* potential, and hence the electronic structure, than a more localized core level ionization. Our experiment uses a newly developed angle-resolving photoelectron-photoion coincidence imaging (AR-PEPICOI) technique and the results are compared with predictions made by a continuum multiple scattering calculation [11] employing  $X\alpha$  local-exchange model potentials (CMS- $X\alpha$ ).

For this preliminary investigation we have chosen to examine the  $5a_1^{-1}$  ionization of CF<sub>3</sub>I (vertical ionization energy  $IE_{\text{vert}} = 13.3$  eV). The resulting ion has two distinct product channels:



with energetic thresholds in Table I. Previous (non-angle-resolved) coincidence measurements taken at various photon energies from threshold up to 21.2 eV have established the existence of pronounced energy dependent electron-ion recoil vector correlations for this system [3,12]. The translational energy release for (1a) indicates an impulsive dissociation mechanism [3] and a large

TABLE I. Accessible dissociative ionization energies (eV).

|  | Threshold energy <sup>a</sup> | Excess energy <sup>b</sup> |
|--|-------------------------------|----------------------------|
| $\text{CF}_3\text{I} \rightarrow \text{CF}_3^+ + \text{I} (^2P_{1/2})$ | 10.91                         | 2.39                       |
| $\text{CF}_3\text{I} \rightarrow \text{CF}_3^+ + \text{I} (^2P_{3/2})$ | 11.85                         | 1.45                       |
| $\text{CF}_3\text{I} \rightarrow \text{I}^+ (^3P_2) + \text{CF}_3$     | 12.70                         | 0.60                       |

<sup>a</sup>0 K values, taken from Ref. [12].<sup>b</sup>At the 13.3 eV  $\bar{A}$  band vertical ionization energy.

photofragment ion anisotropy ( $\beta = 1.25$ ) has been measured for dissociation of an *aligned* parent ion sample (generated *via* a bound-bound excitation to an autoionizing resonance [12]). Hence there is strong evidence to support the assumption of a rapid, axial-recoil ion dissociation in (1a). Similar, though less conclusive, evidence is found for dissociation (1b). This choice of system therefore presents an unusual opportunity to compare alternative fragmentation channels in which the *same* molecular bond (C-I) is broken. We anticipate that, if the above simplifying assumptions—leading to a direct interpretation of the electron-ion recoil correlation as a molecule-frame photoelectron angular distribution—are indeed justified, identical correlations (PADs) should be found. By comparing the channels with each other and with computed PADs we can hope to validate this interpretation of the experimental recoil vector correlations.

The AR-PEPICOI apparatus (Fig. 1) and data reduction techniques employed in this work will be described in detail elsewhere [13] and so are only outlined here. An effusive sample jet is intersected by a monochromatic, collimated beam from an unpolarized HeI (21.22 eV) discharge lamp. When an electron from this approximate point ionization source is detected, ions are extracted in the opposite direction by application of a pulsed source extraction field. Ion-electron pairs from a single molecular ionization event are identified in delayed coincidence

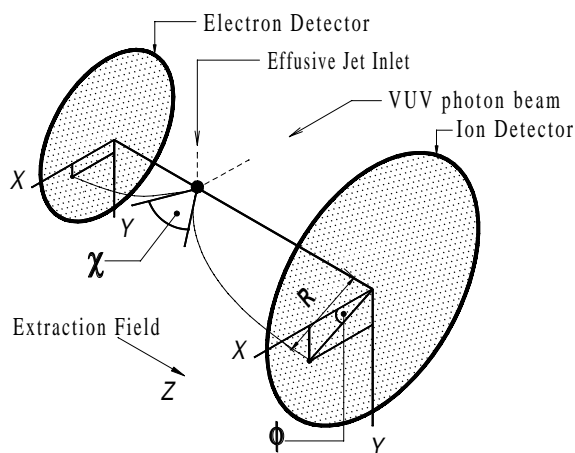


FIG. 1. Schematic of the AR-PEPICOI experiment. Curved electron and ion trajectories from point source to detectors are shown with relevant coordinates indicated.

at fast, position sensitive detectors (psd). The ion flight-time and detector coordinates are used, in conjunction with the known dimensions and imaging characteristics of the gridless ion optics, to infer ion mass and the 3D lab velocity. The initial ion recoil velocity (speed and direction) is then estimated from the latter by subtracting the most probable jet velocity of the parent molecule.

A “Bessel Box” imaging analyzer [14], positioned before the electron psd, is employed to determine the electron recoil velocity. This analyzer is axially symmetric and forms energy-dependent images of its circular entrance slit on the detector plane. Consequently, an electron’s polar recoil angle is fixed by the slit and source geometry, while the energy and azimuthal angle are obtained from the radial and angular coordinates on the electron psd. Transformation to the initial electron recoil velocity is then trivial, as is determination of  $\chi$ , the included angle between the electron and ion recoil directions.

CMS- $X\alpha$  calculations of the  $5a_1^{-1}$  ionization cross section and PADs for this system were performed following procedures described elsewhere [6,15] and using the parameters in Table II. Similar methods have previously been applied to investigate partial ionization cross sections and branching ratios of  $\text{CF}_3\text{I}$  [16]. The calculation needs the light polarization in the molecule frame to be specified. For a randomly oriented molecular ensemble a 2:1 perpendicular:parallel ratio would be expected but is not strictly justified in present circumstances because of preferential sampling of favored lab-frame molecular orientations. This arises because the electron detector does not uniformly sample all lab-frame electron recoil directions and these, we have shown, are correlated with the direction of ion recoil.

The appropriate polarization ratio may be estimated from the experimentally determined distribution of  $\Theta$ , the ion recoil direction about the light propagation direction,  $X$ . Example distributions are shown in Fig. 2 and can be fitted to a Legendre polynomial expansion with coefficients  $C_n$ :

$$F(\Theta) = \frac{1}{4\pi} \sum_{n=0,2,4,\dots} C_n P_n(\cos \Theta). \quad (2)$$

TABLE II. Parameters used in  $\text{CF}_3\text{I}$  CMS- $X\alpha$  calculations.

| Region            | Atomic sphere coordinates <sup>a</sup> (Å) |       |          |        | Final<br>(Initial)<br>State $l_{\max}$ |
|-------------------|--|-------|----------|--------|--|
|                   | $X$  | $Y$   | $Z$      | Radius |  |
| I                 | 0.0  | 0.0   | -0.965   | 1.603  | 5(4)                                   |
| C                 | 0.0  | 0.0   | 1.165    | 0.823  | 4(3)                                   |
| F <sub>1</sub>    | 1.247                                      | 0.0   | 1.634    | 0.897  | 4(2)                                   |
| F <sub>2(3)</sub> | -0.623                                     | 1.080 | (-)1.634 | 0.897  | 4(2)                                   |
| Outer             | 0.0  | 0.0   | 1.007    | 3.575  | 7(5)                                   |

<sup>a</sup> $r_{\text{C-I}} = 2.13 \text{ Å}$ ,  $r_{\text{C-F}} = 1.332 \text{ Å}$ ,  $\angle_{\text{FCF}} = 108.3^\circ$ ,  $\angle_{\text{FCI}} = 110.6^\circ$ .

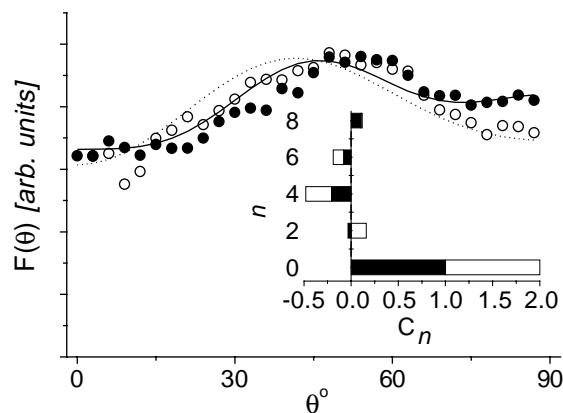


FIG. 2. Example lab recoil distributions,  $F(\Theta)$ : Solid symbols are for  $\text{I}^+$  fragments coincident with 7.7 eV electrons; open symbols are  $\text{I}^+$  with 8.0 eV electrons. Experimental data are fitted with curves, Eq. (2), spanning terms up to  $P_8(\cos \Theta)$ . The inset shows fitted  $C_n$  coefficients. The  $\text{CF}_3^+$  data obtained are all very similar to the 7.7 eV  $\text{I}^+$  data.

The strength of the photon-molecule interaction is proportional to  $|\hat{E} \cdot \hat{\mu}|^2$  and so we seek relative weightings from the mean squared projections of a unit electric vector,  $\hat{E}$ , on the molecule. We define the lab-molecule transformation by rotations of the molecule around the lab axes  $X, Y, Z$ :

$$\mathbf{R}(\Phi, \Theta, \gamma) = R_X(\Phi) R_Y\left(\frac{\pi}{2} + \Theta\right) R_Z(\gamma), \quad (3)$$

where the angle  $\gamma$  specifies the (random) azimuthal orientation of the molecule about its symmetry axis. Hence, choosing any arbitrary direction in the  $YZ$  plane for  $\hat{E}$ , its projection in the molecule frame can be found as

$$\mathbf{e} = \mathbf{R}^{-1} \mathbf{E}. \quad (4)$$

The desired mean values are obtained as

$$\langle e_\alpha^2 \rangle = \int_0^{2\pi} \int_0^{2\pi} \int_0^\pi \frac{1}{2\pi} e_\alpha^2 F(\Theta) \sin \Theta d\Theta d\Phi d\gamma, \quad (5)$$

where  $\alpha$  is one of the molecule-frame coordinates  $x, y, z$ . Only the average over  $\Theta$  needs to be appropriately weighted. The angle  $\Phi$  specifies relative orientation of molecule and polarization vector about  $X$ ; because all polarization directions in the  $ZY$  plane are equivalent a uniform average over  $\Phi$  suffices, as for  $\gamma$ . Combining Eqs. (2)–(5) we find the results

$$\langle e_x^2 \rangle = \langle e_y^2 \rangle = \frac{1}{3} (C_0 + C_2/10), \quad (6a)$$

$$\langle e_z^2 \rangle = \frac{1}{3} (C_0 - C_2/5), \quad (6b)$$

which depend only weakly on the  $P_2$  coefficient. Higher coefficients do not contribute. For the results presented here we find  $C_2/C_0$  lies in the range  $\pm 0.15$  and hence the desired perpendicular:parallel polarization ratios ( $2\langle e_x^2 \rangle : \langle e_z^2 \rangle$ ) vary little from the 2:1 isotropic ratio.

Figure 3 presents our experimental distributions obtained from the electron- $\text{CF}_3^+$  recoil velocity correlation, for a sequence of nominal electron kinetic energies lying in the region of the HeI photoelectron  $\tilde{A}$  band (7.4–8.3 eV). These results have been checked and found to be consistent over a range of different experimental extraction fields. In deriving these distributions we have rejected those coincidence data for which the deduced ion recoil speed is  $< 500 \text{ m s}^{-1}$ ; the experimental uncertainty in the recoil velocity is more pronounced for slower ions and results in far greater errors in the angle  $\chi$ . This causes a smearing out and loss of detail in the distribution  $P(\chi)$ , which appears more isotropic if slow ions are included. Also in Fig. 3 are the corresponding CMS- $X\alpha$  molecule-frame PADs. Since the experiment does not provide azimuthal orientation, these have been averaged over azimuthal angle to allow direct comparison with experimental results.

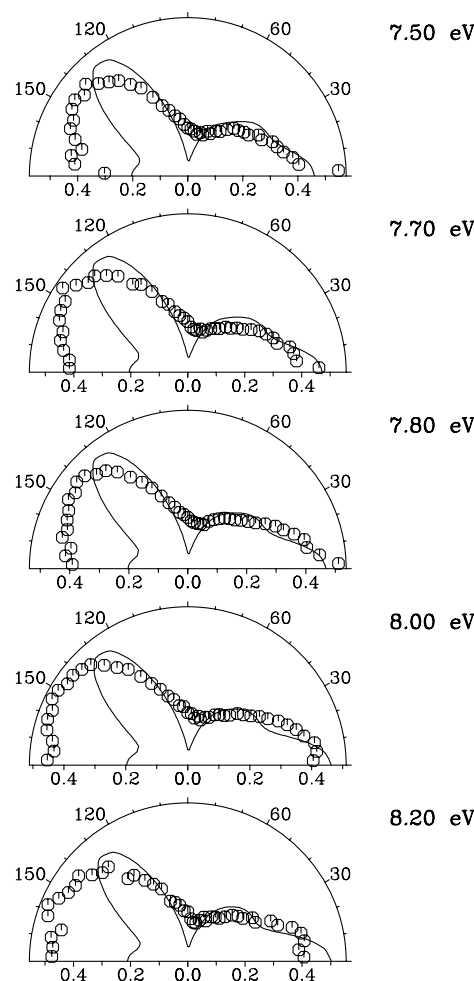


FIG. 3. Polar plots of the electron- $\text{CF}_3^+$  recoil vector correlation,  $P(\chi)$ . Nominal electron kinetic energies are indicated at right. The solid curves are corresponding CMS- $X\alpha$  fixed-molecule PAD calculations. Both experimental and theoretical distributions are arbitrarily scaled for comparison purposes. The  $\text{C} \rightarrow \text{I}$  direction is along  $\chi = 180^\circ$ .

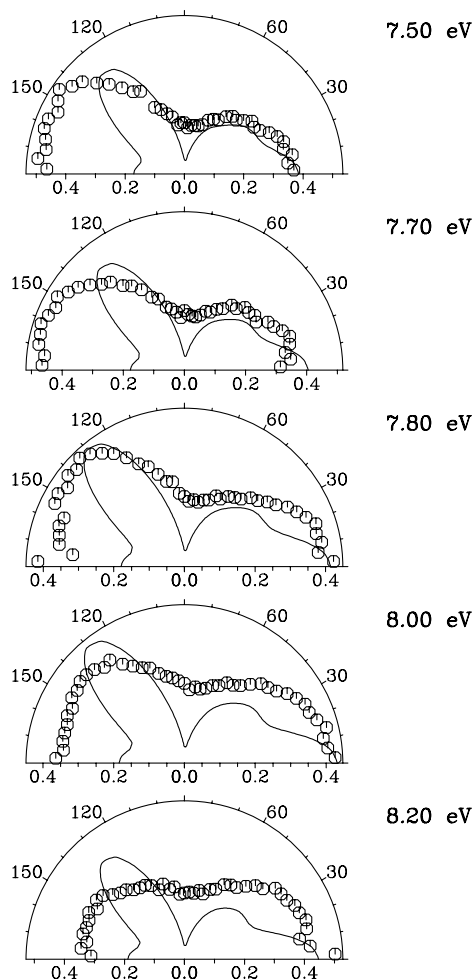


FIG. 4. Electron- $I^+$  recoil correlations,  $P(\chi)$ , and CMS- $X\alpha$  PADs. As Fig. 3, except that  $\chi$  for experimental data has been reflected through  $90^\circ$  so that  $\chi = 180^\circ$  still corresponds to electron recoil in the  $C \rightarrow I$  direction.

The calculated and experimental PADs (Fig. 3) are seen to be similar. Neither varies greatly with kinetic energy and both show principal lobes directed along the  $I \rightarrow CF_3$  direction and off-axis into the I atom hemisphere. While the calculated PAD displays somewhat sharper features, this is not unexpected given the known limitations of the  $X\alpha$  muffin tin potential when calculating ionization cross sections and asymmetry parameters, and overall this must be counted a very encouraging agreement.

Analogous results for the electron- $I^+$  recoil correlation are shown in Fig. 4. At the lower electron kinetic energies the experimentally derived PADs are, as anticipated, essentially identical to the  $CF_3^+$  data in Fig. 3. However, at higher electron kinetic energies the PADs change, tending to a more symmetric, isotropic shape, and are correspondingly in poorer agreement with the CMS- $X\alpha$  calculation. The Lab-frame  $I^+$  distribution,  $F(\Theta)$ , also starts to show some deviation from the  $CF_3^+$  distribution at these higher energies (Fig. 2).

A significant difference between channels (1a) and (1b) is that in the former measurements are made considerably closer to the thermodynamic threshold (Table I) with consequently significant percentage variations of the excess dissociation energy with the studied electron kinetic energy. At a nominal electron energy of 8.2 eV (13 eV ionization energy) there is just a 0.3 eV excess which *all* appears in translation [3,12]; but, since the translational release is near constant, all *additional* energy at higher ionization energies must pass into product vibrational and rotational excitation. We therefore postulate that the observed changes with electron energy in the electron-ion correlation,  $P(\chi)$ , indicate some variation in the underlying ion fragmentation dynamics, specifically a growing relaxation of the axial-recoil limit approximation. With less internal energy the fragmentation presumably becomes more sensitive to the potential near threshold with non-axial forces making a more prominent contribution. The experimental  $P(\chi)$  distribution thus comes to represent a convolution of the molecule-frame PAD with a broader fragment ion angular distribution.

It may be concluded that molecule-frame PADs can be deduced from electron-ion (axial-)recoil vector angular correlations and may also be moderately well reproduced by current photoelectron dynamics calculations. These may *inter alia* help validate the axial-recoil assumption. Under conditions where the recoil vector correlation becomes a more involved convolution of electron and ion fragmentation dynamics it is, at least in principle, possible that information concerning the molecule-frame fragment ion distribution may be deduced with the aid of prior knowledge of the electron angular distribution.

\*Author to whom correspondence should be addressed.

- [1] D. Dill, J. Chem. Phys. **65**, 1130 (1976).
- [2] J.H.D. Eland, J. Chem. Phys. **70**, 2426 (1979).
- [3] K.G. Low, P.D. Hampton, and I. Powis, Chem. Phys. **100**, 401 (1985).
- [4] I. Powis, Chem. Phys. Lett. **189**, 473 (1992).
- [5] I. Powis, J. Chem. Phys. **99**, 3436 (1993).
- [6] I. Powis, J. Chem. Phys. **103**, 5570 (1995).
- [7] A.V. Golovin, N.A. Cherepkov, and V.V. Kuznetsov, Z. Phys. D **24**, 371 (1992).
- [8] E. Shigemasa, J. Adachi, M. Oura, and A. Yagishita, Phys. Rev. Lett. **74**, 359 (1995).
- [9] N. Watanabe *et al.*, Phys. Rev. Lett. **78**, 4910 (1997).
- [10] R.N. Zare, Mol. Photochem. **4**, 1 (1972).
- [11] D. Dill and J.L. Dehmer, J. Chem. Phys. **61**, 692 (1974).
- [12] I. Powis, O. Dutuit, M. Richard-Viard, and P.-M. Guyon, J. Chem. Phys. **92**, 1643 (1990).
- [13] P. Downie and I. Powis (to be published).
- [14] P. Downie, D.J. Reynolds, and I. Powis, Rev. Sci. Instrum. **66**, 3807 (1995).
- [15] I. Powis, J. Chem. Phys. **106**, 5013 (1997).
- [16] B.W. Yates, K.H. Tan, G.M. Bancroft, and J.S. Tse, J. Chem. Phys. **85**, 3840 (1986).